

Evaluation of pretreatment routes for seawater desalination by nanofiltration

Amanda Loreti Hupsel^{ib} ^{a,*}, Cristiano Piacsek Borges^a, Fabiana Valéria da Fonseca^b and Gisele Mattedi Barbosa^a

^a Chemical Engineering Program, COPPE, Federal University of Rio de Janeiro, Horacio Macedo Av, 2030, Technology Center, G-115, University City – 21941450, Rio de Janeiro, RJ, Brazil

^b School of Chemistry, Federal University of Rio de Janeiro, Horacio Macedo Av, 2030, Technology Center, I-124, University City – 21941909, Rio de Janeiro, RJ, Brazil

*Corresponding author. E-mail: ahupsel@peq.coppe.ufrj.br

^{ib} AL, 0000-0001-7688-5077

ABSTRACT

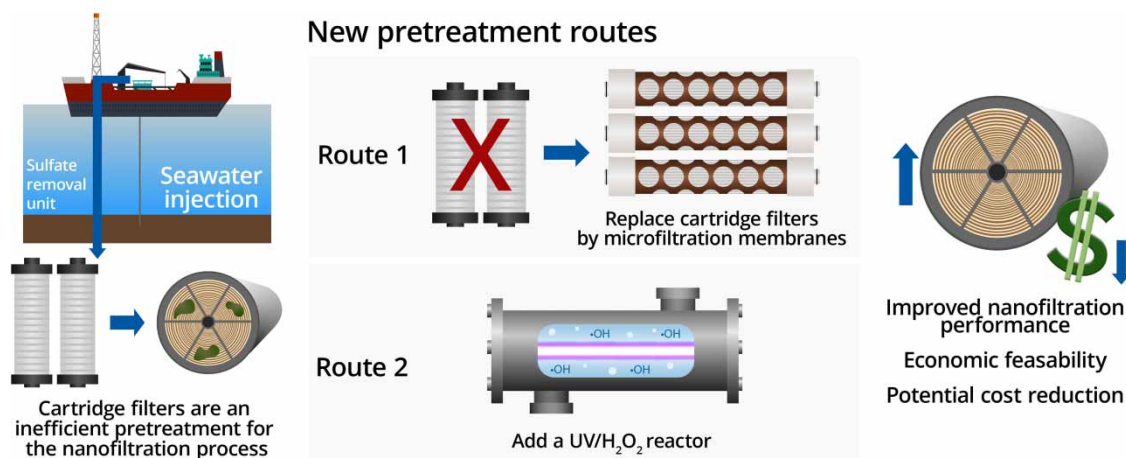
Nanofiltration (NF) has been used as the default sulfate removal process in platforms to treat seawater for water flooding. Seawater is generally pretreated by chlorination and cartridge filters to reduce fouling of the membranes; however, this pretreatment is insufficient to provide water quality high enough to maintain the productivity of the NF membranes. In this study, the performances of two different pretreatment routes were evaluated. Microfiltration (MF) was evaluated as a replacement for cartridge filters, and the advanced oxidation process UV/H₂O₂ was evaluated as an additional stage of pretreatment upstream of the cartridge filters. The permeability of the NF membranes after 12 h of seawater sulfate removal in a bench system was 4.4 L·h⁻¹·m⁻²·bar⁻¹ when the UV/H₂O₂ process was adopted as the pretreatment and 2.9 L·h⁻¹·m⁻²·bar⁻¹ when the MF process was adopted, compared to 1.6 L·h⁻¹·m⁻²·bar⁻¹ achieved for the pretreatment with the cartridge filter alone. These results indicate that NF membrane fouling was significantly higher when seawater was pretreated only by the cartridge filter in comparison to both proposed pretreatments. An economic analysis showed that both systems are economically viable and can potentially reduce the operational costs of the NF sulfate removal process on platforms.

Key words: advanced oxidation process, membrane separation process, microfiltration, nanofiltration, seawater desalination, UV/H₂O₂

HIGHLIGHTS

- Comprehensive analysis of cartridge filters, microfiltration, and advanced oxidation process UV/H₂O₂ pretreatments for seawater desalination by nanofiltration, the last which has not been well stated in the literature.
- UV/H₂O₂ impact on reducing seawater fouling in membranes.
- Economic analysis showing the impact on operational costs of the pretreatments on the nanofiltration sulfate removal process in offshore platforms.

GRAPHICAL ABSTRACT



This is an Open Access article distributed under the terms of the Creative Commons Attribution Licence (CC BY 4.0), which permits copying, adaptation and redistribution, provided the original work is properly cited (<http://creativecommons.org/licenses/by/4.0/>).

1. INTRODUCTION

The formation water in oil reservoirs typically contains alkaline cations, such as calcium, strontium, and barium, which may form highly insoluble and adherent inorganic precipitates when associated with divalent sulfate anions (SO_4^{2-}) present in the seawater injected for oil recovery (Bader 2007; Su *et al.* 2012; Ghasemian *et al.* 2019). Therefore, sulfate removal prior to injection is essential. However, seawater salinity must be partially maintained to preserve the reservoir clay stability. As such, sulfate removal units (SRU) in production platforms employ nanofiltration (NF) membranes that can remove more than 98% of the sulfate from seawater while allowing partial passage of monovalent ions.

The sulfate removal process is initiated by upstream pretreatment, which typically employs cartridge-type filters to remove suspended solids (Moreira *et al.* 2018). Subsequently, pretreated water is pumped into the spiral-wound NF modules, which offer several attractive advantages for sulfate removal, such as low-pressure operation, high flow rates, and relatively low investment, maintenance, and operating costs. However, membranes are also subject to fouling and scaling by microorganisms, suspended solids, and inorganic precipitation.

Fouling is a major challenge in membrane processes that affects membrane performance by decreasing permeate flux, which leads to an increase in feed pressure and, consequently, higher energy consumption. Several studies have also reported that fouling may alter the membrane surface characteristics, thereby affecting salt rejection (Xu *et al.* 2006; Agenson & Urase 2007). Antiscalant agents and biocides can minimize fouling effects; however, their efficiency is limited. The use of chemicals, such as chlorine, for controlling microorganism growth can also be detrimental to NF membranes owing to their low resistance to oxidation. Therefore, periodic chemical cleaning is required to recover the membrane permeate flux, increasing operating costs, and shortening membrane lifetime.

The cleaning frequency is highly dependent on feed quality. Even when properly operated and maintained, conventional cartridge filters do not entirely remove suspended solids and microorganisms, resulting in poor water quality and a high membrane fouling tendency (Jezowska *et al.* 2009). Cartridge filters have other disadvantages, such as frequent replacement and the high volume and weight of the equipment.

Microfiltration (MF) and ultrafiltration (UF) processes have recently been used as alternatives to conventional pretreatment, providing constant and high-quality feed for the sulfate removal process. Membrane filtration has already replaced conventional cartridge filters in some units, and its performance has been reported to improve significantly (Jezowska *et al.* 2009; Pedenaud *et al.* 2012; Alam *et al.* 2017). However, MF and UF processes are generally insufficient for removing natural organic matter (NOM), because of the NOM molecule size (Monnot *et al.* 2016; Winter *et al.* 2016).

NOM is a significant cause of permeate flux decline in processes such as NF and reverse osmosis (RO) for seawater desalination, either by organic deposition or biofouling caused by microorganism growth as a result of dissolved NOM consumption (Song *et al.* 2004; Simon *et al.* 2013; Winter *et al.* 2016). The well-established UV/ H_2O_2 advanced oxidation process could represent an interesting option for NF pretreatment, as it can reduce the NOM content and disinfect seawater. In addition, the UV/ H_2O_2 process is a suitable combination of the NF process owing to its operational simplicity and small-sized systems. This combination was previously used by Song *et al.* (2004) to successfully decrease fouling in groundwater NF (Song *et al.* 2004). Moser *et al.* (2018) also reported mitigation of NF flux decline when an membrane bioreactor (MBR) permeate of petroleum refinery wastewater was pretreated by UV/ H_2O_2 (Moser *et al.* 2018). However, there are few reports on the UV/ H_2O_2 process used prior to seawater desalination or, in fact, the NF process in general.

The reactive ions present in seawater, such as bromide and chloride, may react with hydroxyl radicals and interfere with the application of UV/ H_2O_2 . Nonetheless, according to studies reported by Penru *et al.* (2012), the UV/ H_2O_2 process can promote disinfection and removal of absorbance at 254 nm, associated with the presence of NOM, without the presence of byproducts (Penru *et al.* 2012). Hence, given the UV/ H_2O_2 process capability of degrading NOM, it has a great potential to reduce membrane fouling and improve membrane cleanability, resulting in improved permeate fluxes and a lower frequency of chemical cleaning, which would expand the lifetime of NF membranes.

In this study, two pretreatment routes for seawater sulfate removal were investigated. One route consisted of MF modules coupled to the NF module, and the other consisted of conventional filtration using a cartridge filter, followed by the UV/ H_2O_2 process upstream of the NF system. The permeate flux decline and water recovery degree of the NF were evaluated. The effectiveness of antiscalant agent addition and chemical cleaning was also analyzed. An economic evaluation of the proposed pretreatment routes on an industrial scale was conducted to compare the operating and capital costs to the conventional systems.

2. MATERIAL AND METHODS

2.1. Feedwater characterization

NF desalination was evaluated using synthetic seawater solutions prepared using pure water and analytical-grade salts with the concentrations listed in Table 1, and samples were collected from Guanabara Bay. Seawater samples from Guanabara Bay were collected at different periods, approximately 50 m ahead of the beachfront near the main campus of the Federal University of Rio de Janeiro. The samples were characterized by turbidity (Policontrol AP-2000), ionic conductivity (Quimis Q405M), and total organic carbon (TOC; Shimadzu TOC-V_{CPN}). Modified fouling index (MFI) was measured for all samples to evaluate the fouling tendency. MFI was used instead of the conventional silt density index (SDI) because it has been shown in several studies to be a more accurate and reliable method for measuring membrane fouling.

For the MFI evaluation, water samples were filtered through an MF membrane with a 0.45 µm average pore size (Millipore HAWPO 4700 Type HA) at a constant pressure of 30 psi, according to Schippers and Verdouw method (Schippers & Verdouw 1980). The accumulated filtrated volume is monitored and related to the operation time for the linear region of the generated curve using the following equation.

$$t/V = \alpha + \text{MFI} \times V \quad (1)$$

where V is the accumulated filtered volume (L), t is the operation time, α is the linear coefficient that represents the membrane resistivity, and MFI is the angular coefficient ($\text{s}\cdot\text{L}^{-2}$). An antiscalant agent (GE Hypersperse MDC150, Lenntech) was added to the samples for the NF experiments based on the manufacturer's recommended dosage range of 0.5–4.0 $\text{mg}\cdot\text{L}^{-1}$ for continuous operation. However, the dosage was increased to 10 $\text{mg}\cdot\text{L}^{-1}$ as the concentrate and permeate streams recirculated.

2.2. Membranes

MF membranes were polyimide hollow fibers with 0.4 µm average pore size (PAM Membranas Ltda). The pore size increases from the internal to the outer surface of the fiber, causing filtration to occur toward the fiber lumen. According to the information from the manufacturer, the fibers have a pure water permeability around 200 $\text{L}\cdot\text{h}^{-1}\cdot\text{m}^{-2}\cdot\text{bar}^{-1}$ and a rejection rate of >99% for suspended solids and microorganisms.

The hollow fiber permeation modules were designed for use inside a pressure vessel, as shown in Figure 1. This module configuration employed a permeate collector at the center of the module. The permeate flows from the fiber lumen to the central collector, and the concentrate flows outside the fibers. The central collector can be connected to another module, allowing a serial arrangement. The modules were placed in an acrylic pressure vessel, as shown in Figure 1(b). This setting is similar to that used for commercial NF and RO spiral-wound modules.

Each module was equipped with 252 hollow fibers with a 0.25 m^2 filtration area, providing a total 0.5 m^2 area per vessel. The pilot system contained two parallel pressure vessels, resulting in a total filtration area of 1 m^2 . NF membrane was an NF90-2540 (FILMTEC™) commercial module accommodated in a stainless-steel pressure vessel with a 2.6 m^2 filtration area. Additionally, a sulfate removal membrane (FILMTEC™ SR90-440i) with a filtration area of 28 cm^2 was used in a bench-scale NF system. According to the manufacturer, both NF90-2540 and SR90-440i are TFC membranes with a minimum sulfate rejection of 97 and 99.6%, with permeabilities (2.000 ppm MgSO_4 solution) of 8.7 and 8.32 $\text{L}\cdot\text{h}^{-1}\cdot\text{m}^{-2}\cdot\text{bar}^{-1}$, respectively.

Table 1 | Synthetic seawater composition

salt	Concentration ($\text{mg}\cdot\text{L}^{-1}$)	% of the total
NaCl	23,334	57.9
Na_2SO_4	4,000	9.9
$\text{MgCl}_2\cdot 6\text{H}_2\text{O}$	10,867	26.9
CaCl_2	1,133	2.8
KCl	800	2.0
NaHCO_3	200	0.5

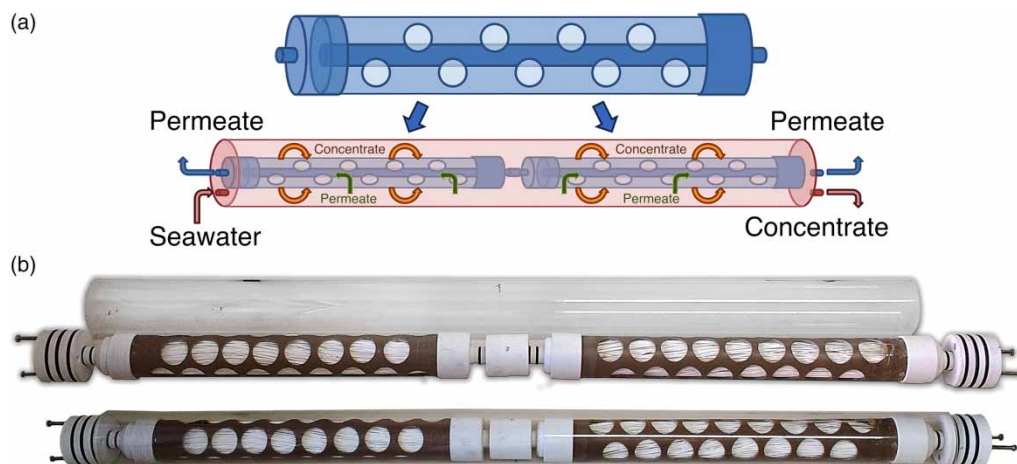


Figure 1 | Schematic (a) and photographs (b) of the module housing and pressure vessel of the MF modules in a serial connection.

The permeate flux decline was monitored until a constant permeability value was achieved for membrane compaction with pure water for all the membranes. The NF and MF membrane integrity was evaluated using $2,000 \text{ mg}\cdot\text{L}^{-1}$ MgSO_4 solutions or suspended solid rejection, respectively. A starch solution (ca. $1 \text{ g}\cdot\text{L}^{-1}$) was used to simulate suspended particulates, and rejection was defined as the ratio between feed water and permeate turbidity.

2.3. UV/ H_2O_2 process

Seawater samples were filtered through a cartridge filter and subjected to the UV/ H_2O_2 process. UV/ H_2O_2 treatment was performed in batch mode in a glass reactor coupled with a thermostatic bath, and the temperature was maintained at approximately 25°C . The UV radiation source was an Hg low-pressure germicidal lamp placed in a quartz sleeve at the center of the reactor. The UV dose was calculated from the exposure time and UV lamp irradiance was measured using a photoradiometer (Delta Ohm HD 2102.2).

Hydrogen peroxide (H_2O_2) at concentrations of 20, 40, 80, 300 and $500 \text{ mg}\cdot\text{L}^{-1}$ were added to the feedwater and recirculation at a $15 \text{ L}\cdot\text{h}^{-1}$ flow rate was conducted until more than 97% of the H_2O_2 added was consumed, to determine both the optimal UV dose and H_2O_2 concentration for organic matter degradation. Higher H_2O_2 concentrations were not evaluated because of the economic issues associated with the treatment.

Feed samples were collected every 30 min for residual H_2O_2 quantification and NOM degradation monitoring. Residual H_2O_2 was measured using the spectrophotometric method with metavanadate, as described elsewhere (Oliveira *et al.* 2001). NOM degradation was evaluated indirectly by measuring the absorbance spectrum decay using a Shimadzu UV-1800 spectrophotometer at wavelengths ranging from 230 to 400 nm. Sodium sulfite solution at $20 \text{ g}\cdot\text{L}^{-1}$ concentration was added to the samples to inactivate H_2O_2 . This procedure is necessary due to the interference of H_2O_2 in the absorption spectrum, which has non-negligible absorbance ($\epsilon_{254\text{nm},\text{H}_2\text{O}_2} = 18.6 \text{ L}\cdot\text{mol}^{-1}\cdot\text{cm}^{-1}$) (Penru *et al.* 2012). The samples generated at the end of each experiment at different H_2O_2 concentrations were subjected to MFI analysis to evaluate their impact on the membrane fouling.

2.4. Membrane experimental set-up and procedures

MF and NF were evaluated in two pilot systems. The systems were built into two aluminum skids, allowing separate or integrated operations. Figure 2 shows the schematic of the two integrated systems. Seawater comes from a water tank and feeds the MF membrane modules into pressure vessels. The permeate may recirculate back to the water tank or be used to feed the NF system. For MF evaluation, the system was operated for 12 h at a transmembrane pressure of 1 bar with permeate and concentrated stream recirculation. The MF membranes were backwashed every 15 min for 35 s. For comparison, the Guanabara Bay water was also pretreated using a conventional SRU cartridge filter.

In the NF system, water was fed from a tank through a high-pressure pump, maintaining the transmembrane pressure at 20 bar. The operation time was varied from 9 to 18 h, and the feed stream was continuously refrigerated to maintain its

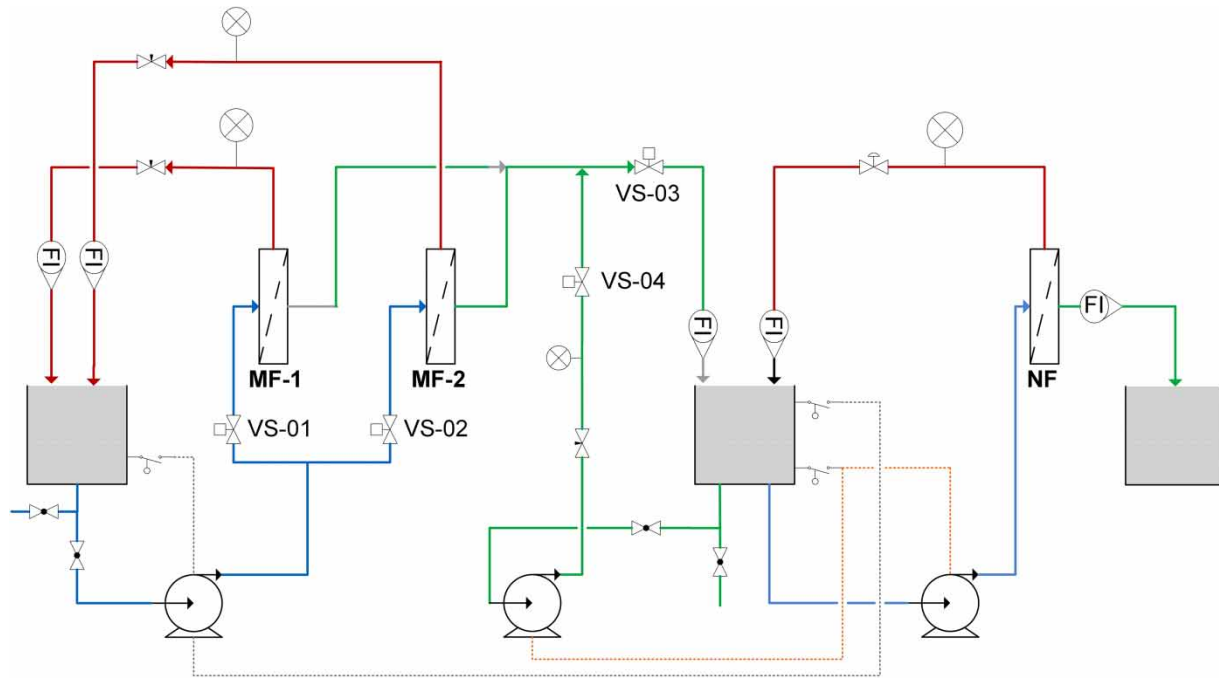


Figure 2 | Schematic diagram of MF- and NF-integrated pilot systems. MF-1 and MF-2 – MF modules; VS-01,02,03 and 04 – electrically activated valves; NF – nanofiltration module; FI – flow indicators.

temperature at approximately 25 °C. The NF was also evaluated on a bench-scale filtration system in a smaller area with an SR90-440i membrane sheet, which is typically employed in SRUs on an industrial scale. This membrane module was not available on a pilot scale.

The performance of the MF and NF processes was evaluated based on the permeate flux decay and water recovery degree. The MF membranes were cleaned with a 100 mg·L⁻¹ NaClO solution recirculating for 4 h. The NF membranes were cleaned by recirculation using a NaOH solution at pH 10 for 30 min and sequentially with a citric acid solution at pH 3 for 90 min. Membrane transport properties were evaluated before and after cleaning to assess the effectiveness of chemical cleaning in recovering the membrane permeability.

2.5. Economic analysis

In order to evaluate the economic feasibility of the processes, the proposed systems were compared with a conventional SRU system that already employs NF membranes, as reported by Weschenfelder *et al.* (2016); Weschenfelder *et al.* 2016). The cost estimate was represented by capital expenditure (CAPEX), operating expenses (OPEX), and total cost (TC) and was normalized per unit volume of treated water, as presented in the following equations.

$$TC = R_{CAPEX} + OPEX \tag{2}$$

$$R_{CAPEX} = (CAPEX / \sum i) / (V_T \cdot n) \tag{3}$$

$$\sum i = \sum 1 / (1 + T_j / 100)^n \tag{4}$$

where R_{CAPEX} is the CAPEX-to-revenue ratio, $\sum i$ is the rate of interest sum, T_j is the annual rate of interest (%), n is the operation period, and V_T is the total volume of treated effluent per year (m³·year⁻¹). CAPEX comprises of the sum of the acquisition costs of the equipment, membrane modules, pressure vessels, valves, piping, and instrumentation apparatus, which constitute a permeation unit. OPEX comprises energy costs, investment depreciation, membrane regeneration and replacement, maintenance, and labor.

The depreciation was calculated according to the straight-line depreciation method, which is defined as the ratio of the fixed investment amount to the period established in the calculation. A period of 20 years and a 12% annual interest rate

were considered. Membranes, UV lamps, and ballast replacements were not included in the estimation and were determined to be independent of operational costs. An SRU with an NF production capacity of $2,000 \text{ m}^3 \cdot \text{h}^{-1}$ seawater treated for injection was considered as the basis of the calculation, continuously operating for 365 day per year. This flow rate was comparable to that of the conventional system used in platforms.

3. RESULTS AND DISCUSSION

3.1. UV/H₂O₂

Several concentrations of H₂O₂ were added to seawater after cartridge filter filtration, and UV radiation was applied until there was less than $2 \text{ mg} \cdot \text{L}^{-1}$ of residual H₂O₂, to investigate the effect of the UV/H₂O₂ process on reducing the seawater fouling potential. The TOC of the seawater sample was $41 \text{ mg} \cdot \text{L}^{-1}$, which is higher than the average seawater concentration, that it is approximately $1 \text{ mg} \cdot \text{L}^{-1}$ (Massé *et al.* 2015). Higher TOC might be related to Guanabara Bay receiving large daily amounts of organic matter and, therefore, having extremely polluted water. Experiments with only the addition of H₂O₂ in a dark environment or UV irradiation without the addition of H₂O₂ were also performed. Figure 3(a) shows the absorbance

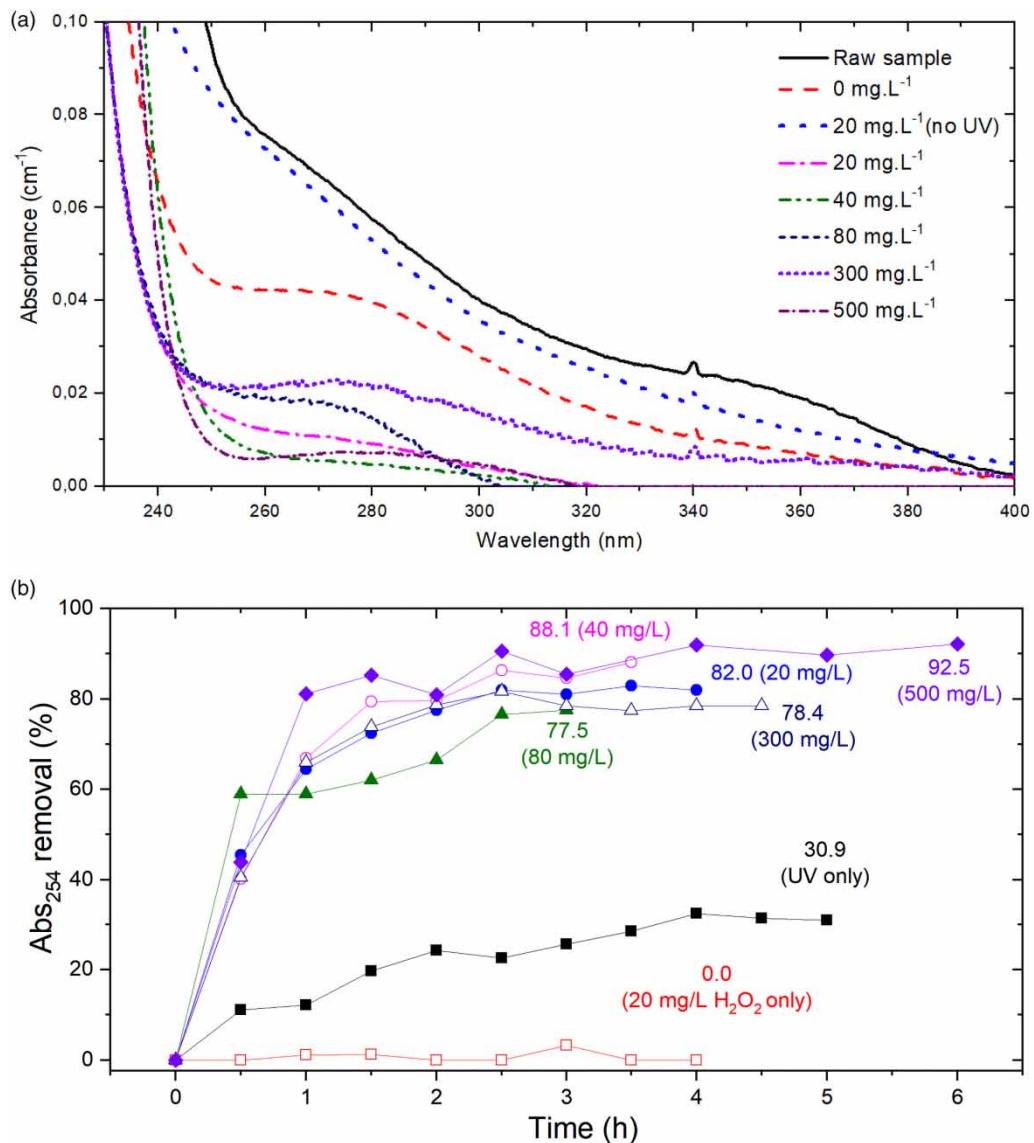


Figure 3 | Absorbance spectra of the samples before and after UV/H₂O₂ experiments (a) and A₂₅₄ removal after UV/H₂O₂ application (b).

spectra from 230 to 400 nm, which are associated with the presence of NOM, at the end of each experiment. Figure 3(b) shows the A_{254} removal throughout the experiments.

The absorbance decay was similar under all conditions in which UV/ H_2O_2 was applied (Figure 3(a)). High degradation was achieved, even at the lowest H_2O_2 concentration. UV irradiation alone was not efficient at completely degrading NOM, whereas the addition of H_2O_2 alone did not result in significant oxidation. Most of the other spectra showed absorbances close to 0, indicating substantial degradation of NOM, especially at concentrations of 40 and 500 $mg\cdot L^{-1}$.

Most of the organic removal was achieved in the early stages of UV/ H_2O_2 experiments (Figure 3(b)). After 2.5 h of irradiation, there were virtually no significant changes in A_{254} . Therefore, the optimum UV irradiation time was defined as 2.5 h, which implies a UV dose of $8.55\text{ kJ}\cdot\text{m}^{-2}$. A_{254} removal did not seem to increase linearly with the H_2O_2 concentration. Several parallel reactions can occur in the UV/ H_2O_2 process depending on the feed concentration, resulting in different percentages of removal at the end of radiation exposure. Nevertheless, it is vital to emphasize that high removal was achieved even at a low concentration of H_2O_2 . The MFI of the seawater treated by UV/ H_2O_2 was determined, and the results are shown in Figure 4.

All H_2O_2 concentrations significantly reduced MFI, indicating that the fouling potential of the samples is closely linked to the NOM concentration. MFI was reduced to 0 at concentrations of 300 and 500 $mg\cdot L^{-1}$, exhibiting the considerable potential of the UV/ H_2O_2 process to improve the performance of seawater NF. As previously discussed, a low H_2O_2 concentration (20 $mg\cdot L^{-1}$) significantly reduced MFI and A_{254} , and considering the economic aspect, it was selected for seawater pretreatment. Thus, the UV/ H_2O_2 process using 20 $mg\cdot L^{-1}$ H_2O_2 and $8.55\text{ kJ}\cdot\text{m}^{-2}$ UV dose was then applied to feed the NF processes.

3.2. Sample characterization

The collected seawater samples showed turbidity values ranging from 7.5 to 13.1 NTU and ionic conductivity ranging from 31.9 to 42.1 $\text{mS}\cdot\text{cm}^{-1}$. MF eliminated the turbidity of the samples. In contrast, samples pretreated with cartridge filters still exhibited turbidity higher than 2 NTU, indicating that suspended solids and microorganisms were not completely removed. A synthetic sample emulating seawater was also prepared, and its conductivity was much higher than that of the collected ones ($63.3\text{ mS}\cdot\text{cm}^{-1}$), because of the dilution of the Guanabara Bay salinity by several river inflows.

The MFI was used to assess the fouling potential. However, the water quality of Guanabara Bay was significantly affected by environmental conditions during sampling, which resulted in a large variation in MFI, as indicated in Table 2. MFI was

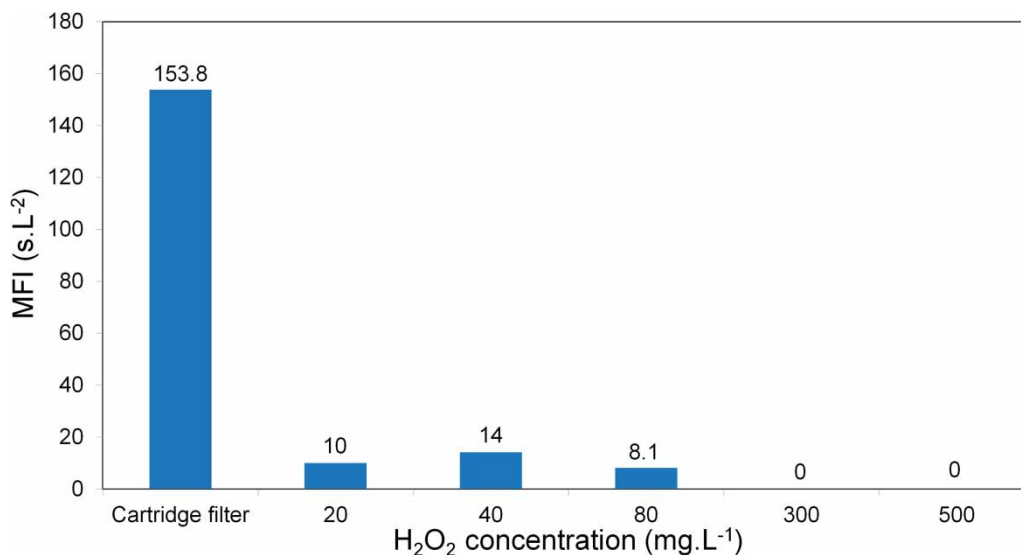


Figure 4 | MFI of treated seawater after cartridge filtration and UV/ H_2O_2 treatment for different H_2O_2 concentrations.

Table 2 | MFI characterization of samples before and after pretreatment routes application

	Untreated sample	Cartridge filter filtrate	Microfiltration permeate	Cartridge filter filtrate + UV/H ₂ O ₂ ^a
Sample 1	16.1	–	0	–
Sample 2	260.2	–	0	–
Sample 3	377.8	153.8	0	10

^aMFI of sample 3 for the dosage of 20 mg·L⁻¹ of H₂O₂ and 8.55 kJ·m⁻² UV.

zero after MF and exhibited a significant decrease after UV/H₂O₂ treatment, which was not achieved by cartridge filter filtration alone.

3.3. MF pretreatment

The performance of the MF process was evaluated by permeate flow decay as a function of the operating time, with total recirculation of both the permeate and concentrate streams. Figure 5 compares the MF results for samples 1 and 2, which

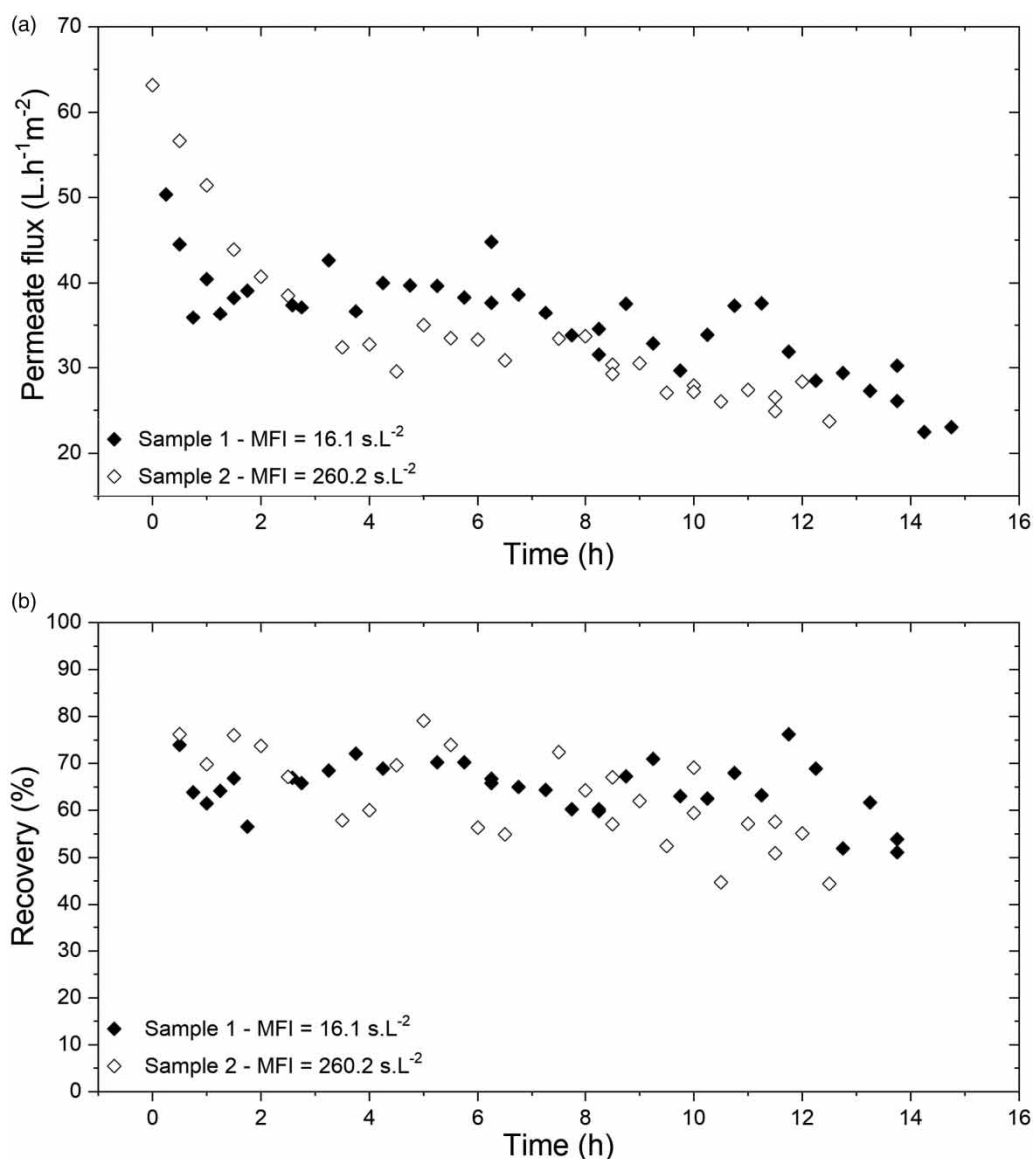


Figure 5 | Microfiltration permeate flux decay (a) and water recovery (b) of samples 1 and 2. Backwashing and filtration: 35 s/15 min. Total recirculation of both permeate and concentrate streams.

exhibited low- and high-fouling indices, respectively. The performance was similar for both feedwaters, indicating that the MF system could operate stably, even with high-fouling index samples.

The initial permeate flux was $\sim 70 \text{ L}\cdot\text{h}^{-1}\cdot\text{m}^{-2}$, stabilizing at approximately $25 \text{ L}\cdot\text{h}^{-1}\cdot\text{m}^{-2}$. The recovery was stable in the 60–70% range in both experiments. It should be mentioned that working with a lower recovery rate can increase the permeate flux and can be used to optimize the design of an industrial unit. The turbidity of the permeate and feed water samples throughout the experiments was measured to evaluate the MF efficiency, and the membrane rejection rate remained above 98% during both processes.

The MF membranes were characterized before and after the experiment. The permeability of the MF membranes in the first characterization was $92.8 \text{ L}\cdot\text{h}^{-1}\cdot\text{m}^2\cdot\text{bar}^{-1}$. Sample 1 MF reduced the membrane permeability to $53.2 \text{ L}\cdot\text{h}^{-1}\cdot\text{m}^2\cdot\text{bar}^{-1}$ (43% reduction). After chemical cleaning, permeability increased to $101.1 \text{ L}\cdot\text{h}^{-1}\cdot\text{m}^2\cdot\text{bar}^{-1}$, indicating that sodium hypochlorite was effective in oxidizing the organic matter that adhered to the membrane surface and consequently recovered the membrane permeate flux.

Similar behavior was observed for membrane characterization after sample 2 MF, as permeability declined from 90.6 to $55.7 \text{ L}\cdot\text{h}^{-1}\cdot\text{m}^2\cdot\text{bar}^{-1}$ (38% reduction) after the experiment, and increased to $103.6 \text{ L}\cdot\text{h}^{-1}\cdot\text{m}^2\cdot\text{bar}^{-1}$ after cleaning. Membrane rejection rates were measured and remained above 98% in all characterizations, demonstrating that chemical cleaning did not cause immediate damage to the membranes, and incrustations caused by seawater were not irreversible. The permeabilities of the cleaned membranes slightly exceeded those of the first characterization, probably because, although the system was rinsed with pure water prior to use in the seawater experiments, the cleaning procedure probably removed the remaining additives or adsorbed materials present in the prior membrane.

3.4. Nanofiltration

NF of synthetic and collected samples was performed using a skid pilot system. The average feed flow was $400 \text{ L}\cdot\text{h}^{-1}$ and the recovery rate was approximately 5% for all tests. The saline rejection rate was evaluated using the permeate and feed ionic conductivity ratios, which were approximately 60–70% in all experiments. However, the sulfate rejection remained higher than 97% when the membranes were characterized using MgSO_4 solutions at $2,000 \text{ mg}\cdot\text{L}^{-1}$ concentration. Figure 6 shows the permeate flux over time normalized to the initial permeate flux for both the synthetic (Figure 6(a)) and collected Guanabara Bay water 3 samples (Figure 6(b)).

For NF of the synthetic sample, the addition of the antiscalant agent resulted in a higher permeate flux, particularly at the end of filtration. The characterization of the NF membranes with MgSO_4 solution showed that the membrane permeability decreased slightly from 6 to $5.7 \text{ L}\cdot\text{h}^{-1}\cdot\text{m}^2\cdot\text{bar}^{-1}$ (5% reduction) after the test performed without the addition of an antiscalant. Acid cleaning increased the permeability to $5.9 \text{ L}\cdot\text{h}^{-1}\cdot\text{m}^2\cdot\text{bar}^{-1}$. Subsequently, an experiment involving the addition of an antiscalant agent was performed. Membrane permeability decreased from 5.9 to $5.4 \text{ L}\cdot\text{h}^{-1}\cdot\text{m}^2\cdot\text{bar}^{-1}$ (an 8% reduction). It was not possible to validate the effectiveness of the antiscalant in synthetic seawater because the reduction in permeability was small. Thus, there were no observable effects on the characterization. Acid cleaning increased the permeability to $5.8 \text{ L}\cdot\text{h}^{-1}\cdot\text{m}^2\cdot\text{bar}^{-1}$, demonstrating that the chemical cleanings were efficient in both tests and were able to recover the permeate flux of the NF membranes, although not completely.

Overall, for the NF experiment with real seawater pretreated by MF, it can be observed in Figure 6(b) that the performance was very similar in both experiments. The permeate flux decreased to approximately 60% of its initial value after 14 h of operation. NF performance was significantly more affected than that in the experiment with synthetic seawater. As the synthetic seawater contained only dissolved salts, the higher reduction in the Guanabara Bay water might be associated with the presence of soluble organic matter.

Membrane permeability decreased from 5.8 to $5.3 \text{ L}\cdot\text{h}^{-1}\cdot\text{m}^2\cdot\text{bar}^{-1}$ (8% reduction) after the experiment with antiscalant addition and from 5.6 to $4.8 \text{ L}\cdot\text{h}^{-1}\cdot\text{m}^2\cdot\text{bar}^{-1}$ (15% reduction) after the experiment without antiscalant. The larger reduction might be associated with the use of the agent in reducing scaling formation. However, the membrane permeability remained similar following alkaline cleaning after the experiment with the antiscalant agent, but it recovered to $5 \text{ L}\cdot\text{h}^{-1}\cdot\text{m}^2\cdot\text{bar}^{-1}$ for the experiment without antiscalant. Acid cleaning was more effective, recovering permeability to $5.6 \text{ L}\cdot\text{h}^{-1}\cdot\text{m}^2\cdot\text{bar}^{-1}$ for both experiments. The rejection rates were above 97% for all characterizations of the NF membranes on the skid system after both synthetic and collected samples nanofiltrations.

Figure 7 shows the NF permeate fluxes for different pretreatments of Guanabara Bay water for the experiment performed in the pilot system (Figure 7(a)) and the experiment performed in the bench system with the SR90-440i membrane (Figure 7(b)).

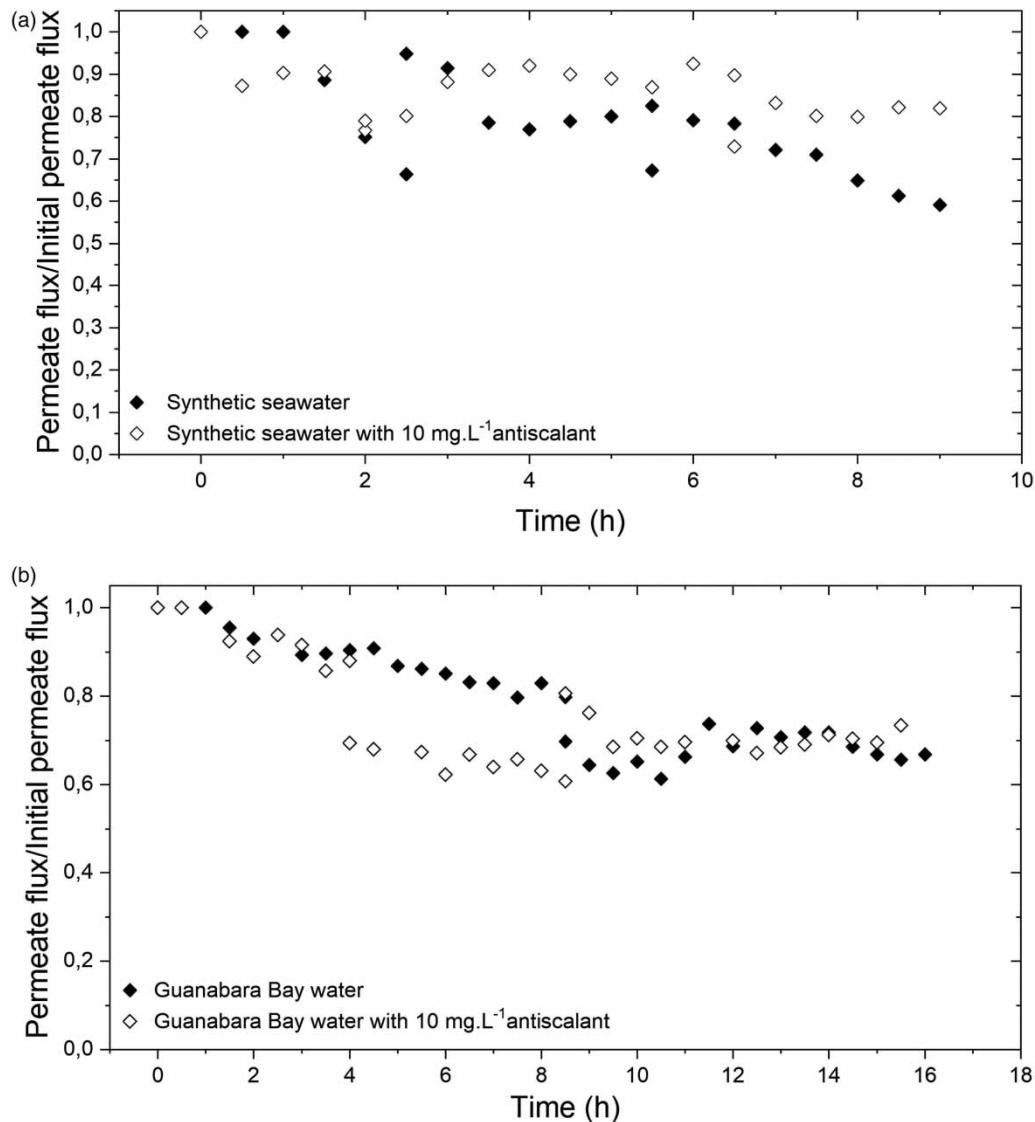


Figure 6 | Normalized permeate flux to initial during nanofiltration of the synthetic sample (a) and Guanabara Bay water sample 3 (MFI = 377.8 s·L⁻²) with microfiltration pretreatment (b), both samples with and without antiscalant agent addition.

In the bench system, the concentrate flow was kept constant at 40 L·h⁻¹ for all the experiments, and the recovery grade was below 1%.

It can be noticed that the permeate flux does not significantly decline with operation time for samples pretreated by cartridge filtration and UV/H₂O₂ for both experiments. On the other hand, when the sample was pretreated by MF or cartridge filtration, an accelerated decline was observed. These results indicate that soluble NOM has a more significant impact on NF membrane performance than suspended solids, as MFI was higher for the UV/H₂O₂ treated sample, as shown in Table 2.

As the membrane area of the bench system was much smaller than that on the pilot scale, the effects on the membrane performance were more pronounced (Figure 7(b)). However, a practically constant permeate flux was achieved during NF of the UV/H₂O₂ pretreated sample, whereas a permeate flux reduction was observed for samples pretreated by other routes. Cartridge filtration as a pretreatment was not efficient in retaining the material responsible for NF membrane fouling, thus resulting in the worst pretreated feed performance. MF was more effective than cartridge filtration, but flux decline was still observed during the experiment. The permeabilities of the NF membranes at the end of each experiment in the bench-

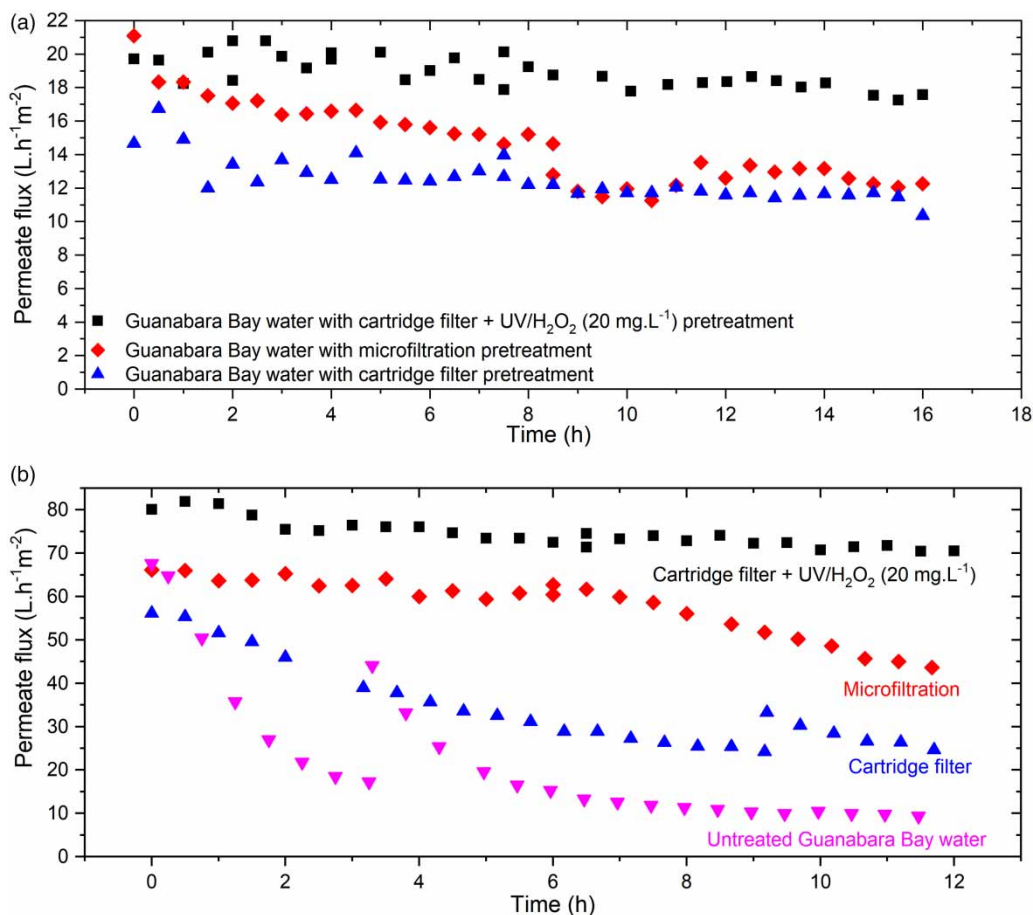


Figure 7 | Permeate flux for nanofiltration of Guanabara Bay water pretreated by various routes in the pilot system using the NF90-2540 membrane (a) and in the bench-scale system using the SR90-440i membrane (b).

scale system were $4.4 \text{ L}\cdot\text{h}^{-1}\cdot\text{m}^{-2}\cdot\text{bar}^{-1}$ for the UV/H₂O₂ feed, $2.9 \text{ L}\cdot\text{h}^{-1}\cdot\text{m}^{-2}\cdot\text{bar}^{-1}$ for the MF feed, $1.6 \text{ L}\cdot\text{h}^{-1}\cdot\text{m}^{-2}\cdot\text{bar}^{-1}$ for the cartridge filtration feed and $0.55 \text{ L}\cdot\text{h}^{-1}\cdot\text{m}^{-2}\cdot\text{bar}^{-1}$ for the untreated feed samples.

The global membrane saline rejection varied between 19 and 25%, but the sulfate rejection rates remained above 97% for all characterizations of the bench-system NF membranes. As such, no effects on the membrane sulfate rejection were observed for the different treatment routes and membranes, as it remained practically constant in all characterizations.

3.5. Economic evaluation

The economic evaluation was based on calculating the CAPEX and OPEX for an SRU, considering the three pretreatment routes studied in the experiments. The main costs associated with SRU implementation and operation are based on the work of Weschenfelder *et al.* (2016). The costs associated with different membrane lifetimes and the implementation of the different pretreatment routes proposed in this study were calculated in comparison with the costs calculated by Weschenfelder *et al.* (2016), who considered the pretreatment to be the conventional cartridge filters.

The costs associated with OPEX estimation require membrane replacement costs, which depend on the membrane's lifetime. Polymeric membranes may endure 5–10 years of operation, according to the main suppliers. The membrane lifetime was established as 5 years for MF membranes and 4 years for NF membranes, according to the usual NF membrane replacement period in the Brazilian SRU. A lifetime of 7 years was also considered for the NF membranes to assess the lifetime cost impact on the economic feasibility of the process. Membrane costs were obtained through an estimate from major suppliers, and the results per cubic meter of treated water ($\text{US\$ m}^{-3}$) are listed in Table 3.

Table 3 | Membranes investment and replacement costs for SRU units

Membrane	Lifetime (year)	Annual replacement cost (US\$)	Unitary cost (US\$.m ⁻³)
MF	5	457,142	0.020
NF	4	938,601	0.054
NF	7	536,343	0.031

Table 4 | Estimated CAPEX for different feed pretreatments of NF units in SRU systems (values in US\$)

	Cartridge filtration	Cartridge filtration + UV/H ₂ O ₂	Microfiltration
Cartridge filters	5,085,948.68	5,085,948.68	–
Nanofiltration skid	8,024,376.65	8,024,376.65	8,024,376.65
Pumps set	3,691,397.35	3,691,397.35	3,691,397.35
Cleaning system	813,165.78	813,165.78	813,165.78
Chemical products injection skid	630,509.33	630,509.33	630,509.33
Electric panel/instrumentation	530,795.98	530,795.98	530,795.98
Membranes set ^a	3,754,404.23	3,754,404.23	6,040,118.52
Technical assistance	542,280.00	542,280.00	542,280.00
Deaerator	4,500,000.00	4,500,000.00	4,500,000.00
MF pretreatment skid	–	–	5,780,000.00
UV system	–	2,417,078.82	–
Total	27,572,878.00	29,989,956.82	30,552,643.61

^aMembrane set cost when MF conducts the feed pretreatment includes both processes, MF and NF.

Equipment and operational costs for an SRU were based on the work of [Weschenfelder et al. \(2016\)](#). The main components present in SRUs were considered for the CAPEX estimation for all pretreatment routes, and their costs are shown in [Table 4](#). The MF unit, MF membranes, and UV unit costs were obtained from major suppliers. The inclusion of the UV system adds a capital cost to the conventional SRU. On the other hand, MF as a pretreatment eliminates cartridge filters, but still exhibits the highest CAPEX, which is related to membrane investment.

For the OPEX evaluation, additional calculations were necessary regarding UV energy consumption, hydrogen peroxide costs, and MF membrane regeneration. The electrical power of the UV unit was estimated according to the optimum dose obtained experimentally (8.55 kJ.m⁻²), resulting in 1.06 × 10⁻² kWh.m⁻³. However, it must be noted that the calculated value refers only to the energy required for the generation of UV radiation with a length of 254 nm. The real energy consumed by the light bulb is higher because, according to the manufacturer, only 30% of the consumed energy is converted to UV radiation. In addition, as the irradiation tends to decrease over time, a factor of 0.7 was adopted, and the final estimated energy consumption was 5.06 × 10⁻² kWh.m⁻³. As the established production capacity is 2,000 m³.h⁻¹, a 101 kW UV reactor is required for treating seawater similar to the samples used in the experiments.

According to [Weschenfelder et al. \(2016\)](#), energy generated in maritime units costs approximately 0.008 US\$.kWh⁻¹. Lamp and ballast replacement costs account for approximately 45% of the total energy cost ([Mahamuni & Adewuyi 2010](#)). The average quotation obtained for a system with these characteristics was US\$ 2,417,078.82, as indicated in [Table 4](#). The hydrogen peroxide cost was calculated from the concentration defined in the experimental stage (20 mg.L⁻¹) and the average quotation value obtained from different suppliers. The resulting value added to the chemical product cost was 0.002 US \$.m⁻³. MF membrane cleaning was considered to occur every cycle of 10 days of operation to calculate MF membrane regeneration costs.

As the proposed pretreatment routes are able to reduce membrane fouling, a higher lifetime for NF membranes was also considered in the calculations, which is an expected consequence of the lower regeneration frequency. Therefore, it was considered 4 years for NF membrane lifetime as observed in actual Brazilian SRU and 7 years as mentioned in the literature,

Table 5 | Estimated OPEX for different feed pretreatments of NF units in SRU systems (values in US\$ · m⁻³)

	Cartridge filtration	Cartridge filtration + UV/H ₂ O ₂ (4 years)	Cartridge filtration + UV/H ₂ O ₂ (7 years)	Microfiltration (4 years)	Microfiltration (7 years)
NF membranes regeneration	0.0130	0.0130	0.0130	0.0130	0.0130
MF membranes regeneration	–	–	–	0.0075	0.0075
Filter replacement	0.0270	0.0270	0.0270	–	–
NF membrane replacement	0.0536	0.0536	0.0306	0.0536	0.0536
MF membrane replacement	–	–	–	0.0261	0.0261
UV lamp/ballast replacement	–	0.0001	0.0001	–	–
Maintenance and manpower	0.0090	0.0090	0.0090	0.0090	0.0090
Chemical products	0.0980	0.1000	0.1000	0.0980	0.0980
Operation energy	0.0010	0.0014	0.0014	0.0010	0.0010
Depreciation	0.0680	0.0735	0.0735	0.0700	0.0700
Total	0.2695	0.2776	0.2546	0.2782	0.2552

when a better pretreatment is applied (Pedenaud *et al.* 2012). Table 5 presents the total OPEX costs per cubic meter of produced injection water (US\$ m⁻³).

If the lifetime of the NF membrane does not change, the OPEX cost estimates result in comparable values for all the considered pretreatment routes. The operating costs for MF and cartridge filtration followed by UV/H₂O₂ treatment were approximately 3% higher than the conventional pretreatment cost. The energy cost of a UV reactor is often a decisive factor in the implementation of commercial units. However, it did not significantly affect the OPEX because of the low cost of energy in offshore units. The higher OPEX for MF can be attributed to membrane replacement.

It is essential to note that, as observed in the experiments, the proposed pretreatments reduced the fouling of the NF membrane and, consequently, the need for membrane cleaning. Thus, a direct impact on the operating costs is expected, reducing the demand for chemicals and increasing the membrane lifetime. For an extended NF membrane lifetime of 7 years, a

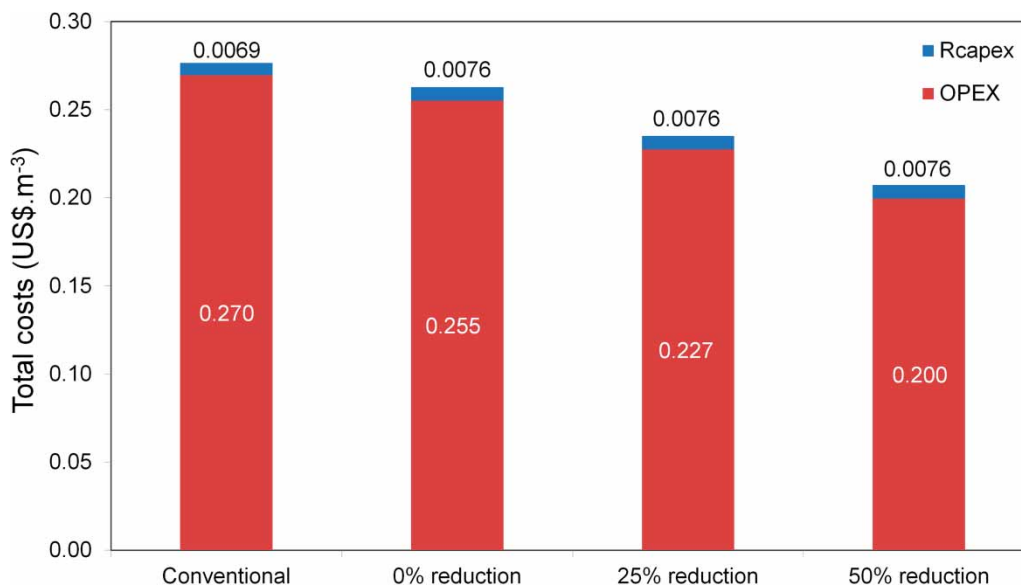


Figure 8 | Comparison of total costs (R_{CAPEX} and OPEX) of conventional SRU system with the proposed MF pretreatment, considering different scenarios for the reduction in chemicals demand. Lifetime of membranes: NF = 7 years; MF = 5 years.

reduction in OPEX was observed for both proposed pretreatment routes, which demonstrates a significant influence on the feasibility of the sulfate removal process. A reduction of about 6% in OPEX was observed for both proposed pretreatment routes.

Figure 8 compares the TC per cubic meter of produced water, replacing the conventional pretreatment with MF. The TC is calculated considering 7 and 5 years for NF and MF membrane replacement, respectively, and a hypothetical reduction of 0, 25, and 50% in demand for chemical products. Similar results for TC were obtained with the addition of UV/H₂O₂ treatment after cartridge filtration and considering 7 years for NF membrane replacement.

As shown in Figure 8, MF pretreatment exhibits a lower cost in all cases, which was also observed in the UV/H₂O₂ route. These results suggest that the replacement of conventional pretreatment by MF or adding a UV system is economically feasible when there is a substantial improvement in the NF operation due to a reduction in the membrane fouling tendency, which may be possible according to the experimental results.

4. CONCLUSIONS

In this work, alternative technologies were proposed for the optimization of pretreatment for the sulfate removal NF process. Two routes were analyzed in comparison to the conventional pretreatment with cartridge filters: the replacement of cartridge filters by MF and the sequential addition of the advanced oxidation process UV/H₂O₂ to the cartridge filters.

The UV/H₂O₂ process was optimized for the collected samples, and characterization showed that both the UV/H₂O₂ and MF processes were effective in reducing the MFI and turbidity of the collected samples. Turbidity reduction was reflected in the NF performance, where higher permeate fluxes were observed compared with conventional pretreatment, both on pilot scale and bench scale. Although MFI was null for MF samples and 10 s·L⁻² for the UV/H₂O₂ treated sample, the UV/H₂O₂ process resulted in better permeate flux in NF compared to the MF sample, which was most noticeable in the bench-scale experiment.

The addition of 10 mg·L⁻¹ antiscalant was slightly useful in preventing scaling of the NF membranes for the synthetic sample during operation. Due to natural sequential dilutions in Guanabara Bay, the collected samples had lower precipitation potential and osmotic pressure. Thus, the permeate flux decay in NF was mainly attributed to the deposition of soluble organic material. It can be inferred that as higher fluxes were obtained for the UV/H₂O₂ process, it was effective in the degradation of these materials.

The evaluated chemical cleanings were suitable to partially recover the permeability of the MF and NF modules, whose membranes remained intact after all operations were performed. However, there was a decrease in permeability throughout the NF processes, indicating that cleaning procedures can be optimized to increase recovery after each process. Regarding the effect of the pretreatments on the chemical cleanings, no significant difference was observed in preliminary studies.

The economic evaluation showed that the improvement in pretreatment could significantly reduce the production cost of the injection water. Both technologies proposed were not only economically feasible but also cheaper in scenarios where the membrane replacement time and quantity of chemical products were minimized, owing to the better performance of NF membranes. However, it should be noted that the implementation of the proposed pretreatments significantly increased CAPEX costs. Nevertheless, this increase would be advantageous given the positive effects considered, which were shown when calculating the total costs (considering R_{CAPEX}).

A global analysis of the studied processes allows us to conclude that the proposed pretreatments are valid and viable technologies for implementation in SRU. The UV/H₂O₂ process proved to be the most effective alternative in both experimental and economic studies, although the TC of the latter was similar for both processes. Experimental studies have shown that the addition of UV/H₂O₂ could significantly improve NF performance in comparison to MF, which would lead to the minimization of chemical product usage and a higher membrane lifetime, increasing economic savings compared to MF replacement. It should also be noted that the studied samples have characteristics that may differ from those of the collected seawater in the SRU because of marine environmental conditions. The characteristics of seawater at great depths may lead to different performances of the studied processes because of the lower organic matter content reported in the literature, which could approximate the effects of MF and UV/H₂O₂ on NF membrane performance offshore. Choosing the MF or UV/H₂O₂ process for a SRU would then depend on the advantages and disadvantages intrinsic to the operation of both processes.

It is important to note that the UV/H₂O₂ process has been poorly described in the literature for application to seawater desalination and presents great potential for pretreatment in other desalination processes, such as reversal osmosis. Its adoption in low NOM water could lead to a reduction in desalination costs, making implementation feasible in many places where reversal osmosis is still too expensive to be used on an industrial scale.

ACKNOWLEDGEMENTS

The authors would like to acknowledge the financial support of Conselho Nacional de Desenvolvimento Científico e Tecnológico (CNPq).

DATA AVAILABILITY STATEMENT

All relevant data are included in the paper or its Supplementary Information.

CONFLICT OF INTEREST

The authors declare there is no conflict.

REFERENCES

- Agenson, K. O. & Urase, T. 2007 Change in membrane performance due to organic fouling in nanofiltration (NF)/reverse osmosis (RO) applications. *Separation and Purification Technology* **55** (2), 147–156.
- Alam, Z., Boczkowski, M., Khoo, S. A., UdhayaRagavan, P. & Chaudhuri, B. 2017 Impact of ultrafiltration on sulfate removal unit recovery, availability and cleaning frequency. In *Offshore Technology Conference*, Texas.
- Bader, M. S. H. 2007 Sulfate removal technologies for oil fields seawater injection operations. *Journal of Petroleum Science and Engineering* **55** (1–2), 93–110.
- Ghasemian, J., Riahi, S., Ayatollahi, S. & Mokhtari, R. 2019 Effect of salinity and ion type on formation damage due to inorganic scale deposition and introducing optimum salinity. *Journal of Petroleum Science and Engineering* **177**, 270–281.
- Jezowska, A., Bottino, A., Capannelli, G., Fabbri, C. & Migliorini, G. 2009 Ultrafiltration as direct pre-treatment of seawater – a case study. *Desalination* **245** (1–3), 723–729.
- Mahamuni, N. N. & Adewuyi, Y. G. 2010 Advanced oxidation processes (AOPs) involving ultrasound for waste water treatment: A review with emphasis on cost estimation. *Ultrasonics Sonochemistry* **17** (6), 990–1003.
- Massé, A., Arab, O., Séchet, V., Jaouen, P., Pontié, M., Sabiri, N. E. & Plantier, S. 2015 Performances of dead-end ultrafiltration of seawater: From the filtration and backwash efficiencies to the membrane fouling mechanisms. *Separation and Purification Technology* **156**, 512–521.
- Monnot, M., Laborie, S. & Cabassud, C. 2016 Granular activated carbon filtration plus ultrafiltration as a pretreatment to seawater desalination lines: Impact on water quality and UF fouling. *Desalination* **383**, 1–11.
- Moreira, A. M. B., Lage, G. G., Tendillo, M. G. S., Zhang, X., Rodrigues, D. & Pessoa, F. 2018 Elimination of fresh water use for chemical cleaning in sulfate removal Units SRU. In: *Proceedings of the Annual Offshore Technology Conference*, Texas. Vol. 1, pp. 459–475.
- Moser, P. B., Ricci, B. C., Reis, B. G., Neta, L. S. F., Cerqueira, A. C. & Amaral, M. C. S. 2018 Effect of MBR-H₂O₂/UV hybrid pre-treatment on nanofiltration performance for the treatment of petroleum refinery wastewater. *Separation and Purification Technology* **192**, 176–184.
- Oliveira, M. C., Pupo Nogueira, R. F., Gomes Neto, J. A., Jardim, W. F. & Rohwedder, J. J. R. 2001 Flow injection spectrophotometric system for hydrogen peroxide monitoring in photo-Fenton degradation processes. *Quimica Nova* **24** (2), 188–190.
- Pedenaud, P., Hurtevent, C. & Baraka-Lokmane, S. 2012 Industrial experience in sea water desulfation. In: *Proceedings of SPE International Conference on Oilfield Scale*, 30–31 May, Aberdeen.
- Penru, Y., Guastalli, A. R., Esplugas, S. & Baig, S. 2012 Application of UV and UV/H₂O₂ to seawater: Disinfection and natural organic matter removal. *Journal of Photochemistry and Photobiology A: Chemistry* **233**, 40–45.
- Schippers, J. C. C. & Verdouw, J. 1980 The modified fouling index, a method of determining the fouling characteristics of water. *Desalination* **32**, 137–148.
- Simon, F. X., Rudé, E., Llorens, J. & Baig, S. 2013 Study on the removal of biodegradable NOM from seawater using biofiltration. *Desalination* **316**, 8–16.
- Song, W., Ravindran, V., Koel, B. E. & Pirbazari, M. 2004 Nanofiltration of natural organic matter with H₂O₂/UV pretreatment: Fouling mitigation and membrane surface characterization. *Journal of Membrane Science* **241** (1), 143–160.
- Su, B., Dou, M., Gao, X., Shang, Y. & Gao, C. 2012 Study on seawater nanofiltration softening technology for offshore oilfield water and polymer flooding. *Desalination* **297**, 30–37.
- Weschenfelder, S. E. E., Fonseca, M. J. C. J. C., Borges, C. P. P. & Campos, J. C. C. 2016 Application of ceramic membranes for water management in offshore oil production platforms: Process design and economics. *Separation and Purification Technology* **171**, 214–220.

- Winter, J., Uhl, W. & Bérubé, P. R. 2016 Integrated oxidation membrane filtration process – NOM rejection and membrane fouling. *Water Research* **104**, 418–424.
- Xu, P., Drewes, J. E., Kim, T. U., Bellona, C. & Amy, G. 2006 Effect of membrane fouling on transport of organic contaminants in NF/RO membrane applications. *Journal of Membrane Science* **279** (1–2), 165–175.

First received 23 October 2023; accepted in revised form 15 December 2023. Available online 8 January 2024